Search for the Rare Decays $B^+ \to D^{(*)+}K_s^0$

B. Aubert,[1] R. Barate,[1] D. Boutigny,[1] F. Couderc,[1] Y. Karyotakis,[1] J. P. Lees,[1] V. Poireau,[1] V. Tisserand,[1]
A. Zghiche,[1] E. Grauges,[2] A. Palano,[3] M. Pappagallo,[3] A. Pompili,[3] J. C. Chen,[4] N. D. Qi,[4] G. Rong,[4] P. Wang,[4]
Y. S. Zhu,[4] G. Eigen,[5] I. Ofte,[5] B. Stugu,[5] G. S. Abrams,[6] M. Battaglia,[6] A. W. Borgland,[6] A. B. Breon,[6]
D. N. Brown,[6] J. Button-Shafer,[6] R. N. Cahn,[6] E. Charles,[6] C. T. Day,[6] M. S. Gill,[6] A. V. Gritsan,[6] Y. Groysman,[6]
R. G. Jacobsen,[6] R. W. Kadel,[6] J. Kadyk,[6] L. T. Kerth,[6] Yu. G. Kolomensky,[6] G. Kukartsev,[6] G. Lynch,[6]
L. M. Mir,[6] P. J. Oddone,[6] T. J. Orimoto,[6] M. Pripstein,[6] N. A. Roe,[6] M. T. Ronan,[6] W. A. Wenzel,[6] M. Barrett,[7]
K. E. Ford,[7] T. J. Harrison,[7] A. J. Hart,[7] C. M. Hawkes,[7] S. E. Morgan,[7] A. T. Watson,[7] M. Fritsch,[8] K. Goetzen,[8]
T. Held,[8] H. Koch,[8] B. Lewandowski,[8] M. Pelizaeus,[8] K. Peters,[8] T. Schroeder,[8] M. Steinke,[8] J. T. Boyd,[9]
J. P. Burke,[9] N. Chevalier,[9] W. N. Cottingham,[9] M. P. Kelly,[9] T. Cuhadar-Donszelmann,[10] C. Hearty,[10]
N. S. Knecht,[10] T. S. Mattison,[10] J. A. McKenna,[10] A. Khan,[11] P. Kyberd,[11] L. Teodorescu,[11] A. E. Blinov,[12]
V. E. Blinov,[12] A. D. Bukin,[12] V. P. Druzhinin,[12] V. B. Golubev,[12] E. A. Kravchenko,[12] A. P. Onuchin,[12]
S. I. Serednyakov,[12] Yu. I. Skovpen,[12] E. P. Solodov,[12] A. N. Yushkov,[12] D. Best,[13] M. Bondioli,[13] M. Bruinsma,[13]
M. Chao,[13] I. Eschrich,[13] D. Kirkby,[13] A. J. Lankford,[13] M. Mandelkern,[13] R. K. Mommsen,[13] W. Roethel,[13]
D. P. Stoker,[13] C. Buchanan,[14] B. L. Hartfiel,[14] A. J. R. Weinstein,[14] S. D. Foulkes,[15] J. W. Gary,[15] O. Long,[15]
B. C. Shen,[15] K. Wang,[15] L. Zhang,[15] D. del Re,[16] H. K. Hadavand,[16] E. J. Hill,[16] D. B. MacFarlane,[16]
H. P. Paar,[16] S. Rahatlou,[16] V. Sharma,[16] J. W. Berryhill,[17] C. Campagnari,[17] A. Cunha,[17] B. Dahmes,[17]
T. M. Hong,[17] A. Lu,[17] M. A. Mazur,[17] J. D. Richman,[17] W. Verkerke,[17] T. W. Beck,[18] A. M. Eisner,[18]
C. J. Flacco,[18] C. A. Heusch,[18] J. Kroseberg,[18] W. S. Lockman,[18] G. Nesom,[18] T. Schalk,[18] B. A. Schumm,[18]
A. Seiden,[18] P. Spradlin,[18] D. C. Williams,[18] M. G. Wilson,[18] J. Albert,[19] E. Chen,[19] G. P. Dubois-Felsmann,[19]
A. Dvoretskii,[19] D. G. Hitlin,[19] I. Narsky,[19] T. Piatenko,[19] F. C. Porter,[19] A. Ryd,[19] A. Samuel,[19] R. Andreassen,[20]
S. Jayatilleke,[20] G. Mancinelli,[20] B. T. Meadows,[20] M. D. Sokoloff,[20] F. Blanc,[21] P. Bloom,[21] S. Chen,[21]
W. T. Ford,[21] U. Nauenberg,[21] A. Olivas,[21] P. Rankin,[21] W. O. Ruddick,[21] J. G. Smith,[21] K. A. Ulmer,[21]
S. R. Wagner,[21] J. Zhang,[21] A. Chen,[22] E. A. Eckhart,[22] A. Soffer,[22] W. H. Toki,[22] R. J. Wilson,[22] Q. Zeng,[22]
E. Feltresi,[23] A. Hauke,[23] B. Spaan,[23] D. Altenburg,[24] T. Brandt,[24] J. Brose,[24] M. Dickopp,[24] V. Klose,[24]
H. M. Lacker,[24] R. Nogowski,[24] S. Otto,[24] A. Petzold,[24] G. Schott,[24] J. Schubert,[24] K. R. Schubert,[24]
R. Schwierz,[24] J. E. Sundermann,[24] D. Bernard,[25] G. R. Bonneaud,[25] P. Grenier,[25] S. Schrenk,[25] Ch. Thiebaux,[25]
G. Vasileiadis,[25] M. Verderi,[25] D. J. Bard,[26] P. J. Clark,[26] W. Gradl,[26] F. Muheim,[26] S. Playfer,[26] Y. Xie,[26]
M. Andreotti,[27] V. Azzolini,[27] D. Bettoni,[27] C. Bozzi,[27] R. Calabrese,[27] G. Cibinetto,[27] E. Luppi,[27] M. Negrini,[27]
L. Piemontese,[27] F. Anulli,[28] R. Baldini-Ferroli,[28] A. Calcaterra,[28] R. de Sangro,[28] G. Finocchiaro,[28] P. Patteri,[28]
I. M. Peruzzi,[28] M. Piccolo,[28] A. Zallo,[28] A. Buzzo,[29] R. Capra,[29] R. Contri,[29] M. Lo Vetere,[29] M. Macri,[29]
M. R. Monge,[29] S. Passaggio,[29] C. Patrignani,[29] E. Robutti,[29] A. Santroni,[29] S. Tosi,[29] S. Bailey,[30]
G. Brandenburg,[30] K. S. Chaisanguanthum,[30] M. Morii,[30] E. Won,[30] R. S. Dubitzky,[31] U. Langenegger,[31]
J. Marks,[31] S. Schenk,[31] U. Uwer,[31] W. Bhimji,[32] D. A. Bowerman,[32] P. D. Dauncey,[32] U. Egede,[32] R. L. Flack,[32]
J. R. Gaillard,[32] G. W. Morton,[32] J. A. Nash,[32] M. B. Nikolich,[32] G. P. Taylor,[32] M. J. Charles,[33] W. F. Mader,[33]
U. Mallik,[33] A. K. Mohapatra,[33] J. Cochran,[34] H. B. Crawley,[34] V. Eyges,[34] W. T. Meyer,[34] S. Prell,[34]
E. I. Rosenberg,[34] A. E. Rubin,[34] J. Yi,[34] N. Arnaud,[35] M. Davier,[35] X. Giroux,[35] G. Grosdidier,[35] A. Höcker,[35]
F. Le Diberder,[35] V. Lepeltier,[35] A. M. Lutz,[35] A. Oyanguren,[35] T. C. Petersen,[35] M. Pierini,[35] S. Plaszczynski,[35]
S. Rodier,[35] P. Roudeau,[35] M. H. Schune,[35] A. Stocchi,[35] G. Wormser,[35] C. H. Cheng,[36] D. J. Lange,[36]
M. C. Simani,[36] D. M. Wright,[36] A. J. Bevan,[37] C. A. Chavez,[37] J. P. Coleman,[37] I. J. Forster,[37] J. R. Fry,[37]
E. Gabathuler,[37] R. Gamet,[37] K. A. George,[37] D. E. Hutchcroft,[37] R. J. Parry,[37] D. J. Payne,[37] K. C. Schofield,[37]
C. Touramanis,[37] C. M. Cormack,[38] F. Di Lodovico,[38] R. Sacco,[38] C. L. Brown,[39] G. Cowan,[39] H. U. Flaecher,[39]
M. G. Green,[39] D. A. Hopkins,[39] P. S. Jackson,[39] T. R. McMahon,[39] S. Ricciardi,[39] F. Salvatore,[39] D. Brown,[40]
C. L. Davis,[40] J. Allison,[41] N. R. Barlow,[41] R. J. Barlow,[41] M. C. Hodgkinson,[41] G. D. Lafferty,[41] M. T. Naisbit,[41]
J. C. Williams,[41] C. Chen,[42] A. Farbin,[42] W. D. Hulsbergen,[42] A. Jawahery,[42] D. Kovalskyi,[42] C. K. Lae,[42]
V. Lillard,[42] D. A. Roberts,[42] G. Simi,[42] G. Blaylock,[43] C. Dallapiccola,[43] S. S. Hertzbach,[43] R. Kofler,[43]
V. B. Koptchev,[43] X. Li,[43] T. B. Moore,[43] S. Saremi,[43] H. Staengle,[43] S. Willocq,[43] R. Cowan,[44] K. Koeneke,[44]
G. Sciolla,[44] S. J. Sekula,[44] F. Taylor,[44] R. K. Yamamoto,[44] H. Kim,[45] P. M. Patel,[45] S. H. Robertson,[45]

A. Lazzaro,[46] V. Lombardo,[46] F. Palombo,[46] J. M. Bauer,[47] L. Cremaldi,[47] V. Eschenburg,[47] R. Godang,[47] R. Kroeger,[47] J. Reidy,[47] D. A. Sanders,[47] D. J. Summers,[47] H. W. Zhao,[47] S. Brunet,[48] D. Côté,[48] P. Taras,[48] B. Viaud,[48] H. Nicholson,[49] N. Cavallo,[50, *] G. De Nardo,[50] F. Fabozzi,[50, *] C. Gatto,[50] L. Lista,[50] D. Monorchio,[50] P. Paolucci,[50] D. Piccolo,[50] C. Sciacca,[50] M. Baak,[51] H. Bulten,[51] G. Raven,[51] H. L. Snoek,[51] L. Wilden,[51] C. P. Jessop,[52] J. M. LoSecco,[52] T. Allmendinger,[53] G. Benelli,[53] K. K. Gan,[53] K. Honscheid,[53] D. Hufnagel,[53] P. D. Jackson,[53] H. Kagan,[53] R. Kass,[53] T. Pulliam,[53] A. M. Rahimi,[53] R. Ter-Antonyan,[53] Q. K. Wong,[53] J. Brau,[54] R. Frey,[54] O. Igonkina,[54] M. Lu,[54] C. T. Potter,[54] N. B. Sinev,[54] D. Strom,[54] E. Torrence,[54] F. Colecchia,[55] A. Dorigo,[55] F. Galeazzi,[55] M. Margoni,[55] M. Morandin,[55] M. Posocco,[55] M. Rotondo,[55] F. Simonetto,[55] R. Stroili,[55] C. Voci,[55] M. Benayoun,[56] H. Briand,[56] J. Chauveau,[56] P. David,[56] L. Del Buono,[56] Ch. de la Vaissière,[56] O. Hamon,[56] M. J. J. John,[56] Ph. Leruste,[56] J. Malclès,[56] J. Ocariz,[56] L. Roos,[56] G. Therin,[56] P. K. Behera,[57] L. Gladney,[57] Q. H. Guo,[57] J. Panetta,[57] M. Biasini,[58] R. Covarelli,[58] S. Pacetti,[58] M. Pioppi,[58] C. Angelini,[59] G. Batignani,[59] S. Bettarini,[59] F. Bucci,[59] G. Calderini,[59] M. Carpinelli,[59] R. Cenci,[59] F. Forti,[59] M. A. Giorgi,[59] A. Lusiani,[59] G. Marchiori,[59] M. Morganti,[59] N. Neri,[59] E. Paoloni,[59] M. Rama,[59] G. Rizzo,[59] J. Walsh,[59] M. Haire,[60] D. Judd,[60] K. Paick,[60] D. E. Wagoner,[60] J. Biesiada,[61] N. Danielson,[61] P. Elmer,[61] Y. P. Lau,[61] C. Lu,[61] J. Olsen,[61] A. J. S. Smith,[61] A. V. Telnov,[61] F. Bellini,[62] G. Cavoto,[62] A. D'Orazio,[62] E. Di Marco,[62] R. Faccini,[62] F. Ferrarotto,[62] F. Ferroni,[62] M. Gaspero,[62] L. Li Gioi,[62] M. A. Mazzoni,[62] S. Morganti,[62] G. Piredda,[62] F. Polci,[62] F. Safai Tehrani,[62] C. Voena,[62] H. Schröder,[63] G. Wagner,[63] R. Waldi,[63] T. Adye,[64] N. De Groot,[64] B. Franek,[64] G. P. Gopal,[64] E. O. Olaiya,[64] F. F. Wilson,[64] R. Aleksan,[65] S. Emery,[65] A. Gaidot,[65] S. F. Ganzhur,[65] P.-F. Giraud,[65] G. Graziani,[65] G. Hamel de Monchenault,[65] W. Kozanecki,[65] M. Legendre,[65] G. W. London,[65] B. Mayer,[65] G. Vasseur,[65] Ch. Yèche,[65] M. Zito,[65] M. V. Purohit,[66] A. W. Weidemann,[66] J. R. Wilson,[66] F. X. Yumiceva,[66] T. Abe,[67] M. T. Allen,[67] D. Aston,[67] R. Bartoldus,[67] N. Berger,[67] A. M. Boyarski,[67] O. L. Buchmueller,[67] R. Claus,[67] M. R. Convery,[67] M. Cristinziani,[67] J. C. Dingfelder,[67] D. Dong,[67] J. Dorfan,[67] D. Dujmic,[67] W. Dunwoodie,[67] S. Fan,[67] R. C. Field,[67] T. Glanzman,[67] S. J. Gowdy,[67] T. Hadig,[67] V. Halyo,[67] C. Hast,[67] T. Hryn'ova,[67] W. R. Innes,[67] M. H. Kelsey,[67] P. Kim,[67] M. L. Kocian,[67] D. W. G. S. Leith,[67] J. Libby,[67] S. Luitz,[67] V. Luth,[67] H. L. Lynch,[67] H. Marsiske,[67] R. Messner,[67] D. R. Muller,[67] C. P. O'Grady,[67] V. E. Ozcan,[67] A. Perazzo,[67] M. Perl,[67] B. N. Ratcliff,[67] A. Roodman,[67] A. A. Salnikov,[67] R. H. Schindler,[67] J. Schwiening,[67] A. Snyder,[67] J. Stelzer,[67] J. Strube,[54, 67] D. Su,[67] M. K. Sullivan,[67] K. Suzuki,[67] S. Swain,[67] J. M. Thompson,[67] J. Va'vra,[67] M. Weaver,[67] W. J. Wisniewski,[67] M. Wittgen,[67] D. H. Wright,[67] A. K. Yarritu,[67] K. Yi,[67] C. C. Young,[67] P. R. Burchat,[68] A. J. Edwards,[68] S. A. Majewski,[68] B. A. Petersen,[68] C. Roat,[68] M. Ahmed,[69] S. Ahmed,[69] M. S. Alam,[69] J. A. Ernst,[69] M. A. Saeed,[69] M. Saleem,[69] F. R. Wappler,[69] S. B. Zain,[69] W. Bugg,[70] M. Krishnamurthy,[70] S. M. Spanier,[70] R. Eckmann,[71] J. L. Ritchie,[71] A. Satpathy,[71] R. F. Schwitters,[71] J. M. Izen,[72] I. Kitayama,[72] X. C. Lou,[72] S. Ye,[72] F. Bianchi,[73] M. Bona,[73] F. Gallo,[73] D. Gamba,[73] M. Bomben,[74] L. Bosisio,[74] C. Cartaro,[74] F. Cossutti,[74] G. Della Ricca,[74] S. Dittongo,[74] S. Grancagnolo,[74] L. Lanceri,[74] P. Poropat,[74, †] L. Vitale,[74] F. Martinez-Vidal,[75] R. S. Panvini,[76, †] Sw. Banerjee,[77] B. Bhuyan,[77] C. M. Brown,[77] D. Fortin,[77] K. Hamano,[77] R. Kowalewski,[77] J. M. Roney,[77] R. J. Sobie,[77] J. J. Back,[78] P. F. Harrison,[78] T. E. Latham,[78] G. B. Mohanty,[78] H. R. Band,[79] X. Chen,[79] B. Cheng,[79] S. Dasu,[79] M. Datta,[79] A. M. Eichenbaum,[79] K. T. Flood,[79] M. Graham,[79] J. J. Hollar,[79] J. R. Johnson,[79] P. E. Kutter,[79] H. Li,[79] R. Liu,[79] B. Mellado,[79] A. Mihalyi,[79] Y. Pan,[79] R. Prepost,[79] P. Tan,[79] J. H. von Wimmersperg-Toeller,[79] J. Wu,[79] S. L. Wu,[79] Z. Yu,[79] M. G. Greene,[80] and H. Neal[80]

(The *BABAR* Collaboration)

[1]*Laboratoire de Physique des Particules, F-74941 Annecy-le-Vieux, France*
[2]*IFAE, Universitat Autonoma de Barcelona, E-08193 Bellaterra, Barcelona, Spain*
[3]*Università di Bari, Dipartimento di Fisica and INFN, I-70126 Bari, Italy*
[4]*Institute of High Energy Physics, Beijing 100039, China*
[5]*University of Bergen, Inst. of Physics, N-5007 Bergen, Norway*
[6]*Lawrence Berkeley National Laboratory and University of California, Berkeley, California 94720, USA*
[7]*University of Birmingham, Birmingham, B15 2TT, United Kingdom*
[8]*Ruhr Universität Bochum, Institut für Experimentalphysik 1, D-44780 Bochum, Germany*
[9]*University of Bristol, Bristol BS8 1TL, United Kingdom*
[10]*University of British Columbia, Vancouver, British Columbia, Canada V6T 1Z1*
[11]*Brunel University, Uxbridge, Middlesex UB8 3PH, United Kingdom*
[12]*Budker Institute of Nuclear Physics, Novosibirsk 630090, Russia*
[13]*University of California at Irvine, Irvine, California 92697, USA*
[14]*University of California at Los Angeles, Los Angeles, California 90024, USA*

[15] University of California at Riverside, Riverside, California 92521, USA

[16] University of California at San Diego, La Jolla, California 92093, USA

[17] University of California at Santa Barbara, Santa Barbara, California 93106, USA

[18] University of California at Santa Cruz, Institute for Particle Physics, Santa Cruz, California 95064, USA

[19] California Institute of Technology, Pasadena, California 91125, USA

[20] University of Cincinnati, Cincinnati, Ohio 45221, USA

[21] University of Colorado, Boulder, Colorado 80309, USA

[22] Colorado State University, Fort Collins, Colorado 80523, USA

[23] Universität Dortmund, Institut fur Physik, D-44221 Dortmund, Germany

[24] Technische Universität Dresden, Institut für Kern- und Teilchenphysik, D-01062 Dresden, Germany

[25] Ecole Polytechnique, LLR, F-91128 Palaiseau, France

[26] University of Edinburgh, Edinburgh EH9 3JZ, United Kingdom

[27] Università di Ferrara, Dipartimento di Fisica and INFN, I-44100 Ferrara, Italy

[28] Laboratori Nazionali di Frascati dell'INFN, I-00044 Frascati, Italy

[29] Università di Genova, Dipartimento di Fisica and INFN, I-16146 Genova, Italy

[30] Harvard University, Cambridge, Massachusetts 02138, USA

[31] Universität Heidelberg, Physikalisches Institut, Philosophenweg 12, D-69120 Heidelberg, Germany

[32] Imperial College London, London, SW7 2AZ, United Kingdom

[33] University of Iowa, Iowa City, Iowa 52242, USA

[34] Iowa State University, Ames, Iowa 50011-3160, USA

[35] Laboratoire de l'Accélérateur Linéaire, F-91898 Orsay, France

[36] Lawrence Livermore National Laboratory, Livermore, California 94550, USA

[37] University of Liverpool, Liverpool L69 7ZE, United Kingdom

[38] Queen Mary, University of London, E1 4NS, United Kingdom

[39] University of London, Royal Holloway and Bedford New College, Egham, Surrey TW20 0EX, United Kingdom

[40] University of Louisville, Louisville, Kentucky 40292, USA

[41] University of Manchester, Manchester M13 9PL, United Kingdom

[42] University of Maryland, College Park, Maryland 20742, USA

[43] University of Massachusetts, Amherst, Massachusetts 01003, USA

[44] Massachusetts Institute of Technology, Laboratory for Nuclear Science, Cambridge, Massachusetts 02139, USA

[45] McGill University, Montréal, Quebec, Canada H3A 2T8

[46] Università di Milano, Dipartimento di Fisica and INFN, I-20133 Milano, Italy

[47] University of Mississippi, University, Mississippi 38677, USA

[48] Université de Montréal, Laboratoire René J. A. Lévesque, Montréal, Quebec, Canada H3C 3J7

[49] Mount Holyoke College, South Hadley, Massachusetts 01075, USA

[50] Università di Napoli Federico II, Dipartimento di Scienze Fisiche and INFN, I-80126, Napoli, Italy

[51] NIKHEF, National Institute for Nuclear Physics and High Energy Physics, NL-1009 DB Amsterdam, The Netherlands

[52] University of Notre Dame, Notre Dame, Indiana 46556, USA

[53] Ohio State University, Columbus, Ohio 43210, USA

[54] University of Oregon, Eugene, Oregon 97403, USA

[55] Università di Padova, Dipartimento di Fisica and INFN, I-35131 Padova, Italy

[56] Universités Paris VI et VII, Laboratoire de Physique Nucléaire et de Hautes Energies, F-75252 Paris, France

[57] University of Pennsylvania, Philadelphia, Pennsylvania 19104, USA

[58] Università di Perugia, Dipartimento di Fisica and INFN, I-06100 Perugia, Italy

[59] Università di Pisa, Dipartimento di Fisica, Scuola Normale Superiore and INFN, I-56127 Pisa, Italy

[60] Prairie View A&M University, Prairie View, Texas 77446, USA

[61] Princeton University, Princeton, New Jersey 08544, USA

[62] Università di Roma La Sapienza, Dipartimento di Fisica and INFN, I-00185 Roma, Italy

[63] Universität Rostock, D-18051 Rostock, Germany

[64] Rutherford Appleton Laboratory, Chilton, Didcot, Oxon, OX11 0QX, United Kingdom

[65] DSM/Dapnia, CEA/Saclay, F-91191 Gif-sur-Yvette, France

[66] University of South Carolina, Columbia, South Carolina 29208, USA

[67] Stanford Linear Accelerator Center, Stanford, California 94309, USA

[68] Stanford University, Stanford, California 94305-4060, USA

[69] State University of New York, Albany, New York 12222, USA

[70] University of Tennessee, Knoxville, Tennessee 37996, USA

[71] University of Texas at Austin, Austin, Texas 78712, USA

[72] University of Texas at Dallas, Richardson, Texas 75083, USA

[73] Università di Torino, Dipartimento di Fisica Sperimentale and INFN, I-10125 Torino, Italy

[74] Università di Trieste, Dipartimento di Fisica and INFN, I-34127 Trieste, Italy

[75] IFIC, Universitat de Valencia-CSIC, E-46071 Valencia, Spain

[76] Vanderbilt University, Nashville, Tennessee 37235, USA

[77] University of Victoria, Victoria, British Columbia, Canada V8W 3P6

[78] Department of Physics, University of Warwick, Coventry CV4 7AL, United Kingdom

[79] *University of Wisconsin, Madison, Wisconsin 53706, USA*
[80] *Yale University, New Haven, Connecticut 06511, USA*

We report on the search for the rare decays $B^+ \to D^{(*)+}K_s^0$ in approximately 226 million $\Upsilon(4S) \to B\overline{B}$ decays collected with the *BABAR* detector at the PEP-II asymmetric-energy B factory at SLAC. We do not observe any significant signal and we set 90% confidence level upper limits on the branching fractions, $\mathcal{B}(B^+ \to D^+K^0) < 0.5 \times 10^{-5}$ and $\mathcal{B}(B^+ \to D^{*+}K^0) < 0.9 \times 10^{-5}$.

Meson decays in which neither constituent quark appears in the final state are expected to be dominated by annihilation diagrams, in which the two quarks interact directly. Such processes provide interesting insights into the internal dynamics of B mesons and need to be understood to make precise predictions on B meson decays. Such diagrams cannot be calculated by assuming factorization since both the quarks play a role and a reliable theoretical prediction for the corresponding amplitudes does not exist. These amplitudes are expected to be suppressed with respect to amplitudes where one of the two quarks is a spectator by a factor $\sim f_B/m_B \sim 0.04$ ($f_B \sim 200$ MeV and $m_B = 5.28$ GeV/c^2 are the B meson decay constant [1] and mass, respectively). This factor represents the amplitude for the two quark wave functions overlapping, a necessary condition in annihilations. So far no process relying entirely on annihilation has been observed and the assumption that these types of diagrams can be neglected is frequently used in theoretical calculations. Some studies [2] indicate, though, that processes with a spectator quark can contribute to annihilation-mediated decays by *rescattering* if the final state is reached in two steps: a decay into two mesons that can occur with a spectator quark, and a subsequent strong interaction between the two mesons which produces the final state of interest. Figure 1 shows the Feynman diagram for the decays $B^+ \to D^{(*)+}K_s^0$ and $B^+ \to D_s^+\pi^0$ [3], and the hadron-level diagram for the rescattering. Strong rescattering could then mimic large contributions from annihilation diagrams to the level of not being negligible any more.

The decays $B^+ \to D^{(*)+}K_s^0$ are particularly suited to study annihilations because of their relatively clean experimental signature and because their branching fractions are expected to be at the level of the current sensitivity (10^{-5}) if large rescattering occurs, or three orders of magnitude below if not [2]. Moreover the branching fraction of these decays can be used to constrain the annihilation amplitudes in the phenomenological fits [4] that allows to translate the measurement of the amplitude of $B^+ \to D^0K^+$ into estimates of the Cabibbo-suppressed decay $B^0 \to D^0K^0$ needed in some CP measurements [5]. Neither of the modes studied here has been observed so far, and a 90% confidence level upper limit on the branching fraction $\mathcal{B}(B^+ \to D^{*+}K^0) < 9.5 \times 10^{-5}$ has been established by CLEO [6].

In this paper we present the results of the search for $B^+ \to D^{(*)+}K_s^0$ decays in 225.9 ± 2.5 million $\Upsilon(4S) \to B\overline{B}$ decays, collected with the *BABAR* detector [7] at the PEP-II asymmetric-energy B factory at SLAC. We use a Monte Carlo (MC) simulation of the *BABAR* detector based on GEANT4 [8] to validate the analysis procedure, estimate efficiencies, and to study the relevant backgrounds. We also use 12.4 fb^{-1} of data collected at a center-of-mass energy approximately 40 MeV below the $\Upsilon(4S)$ mass.

Candidates for D^+ mesons are reconstructed in the modes $D^+ \to K^-\pi^+\pi^+$ and $D^+ \to K_s^0\pi^+$. Candidates for D^{*+} mesons are reconstructed in the mode $D^{*+} \to D^0\pi^+$, where the D^0 subsequently decays to one of the four modes $K^-\pi^+$, $K^-\pi^+\pi^0$, $K^-\pi^+\pi^-\pi^+$, or $K_s^0\pi^+\pi^-$.

K_s^0 candidates are reconstructed from two oppositely-charged tracks with an invariant mass $491 < m_{\pi^+\pi^-} < 504$ MeV/c^2 (corresponding to a ±2 standard deviations, σ, window around the mean value in control samples). The χ^2 of the $\pi^+\pi^-$ vertex fit must have a probability greater than 0.1% and the K_s^0 flight distance from the primary vertex in the plane transverse to the beam axis in the event must be greater than 2 mm. Kaons and pions coming from the D are required to have momentum in the laboratory frame greater than 200 MeV/c and 150 MeV/c, respectively, except in the decays $D^0 \to K^-\pi^+$ ($K^-\pi^+\pi^0$) where the momentum threshold for both the tracks is 200 (150) MeV/c. To identify charged kaons we use a selection with an efficiency of 95% and a 12% pion misidentification probability. π^0 candidates are reconstructed combining two photons with invariant mass $120 < m_{\gamma\gamma} < 150$ MeV/c^2 (corresponding to a $\pm2\sigma$ window around the mean value estimated on control samples) and a minimum total energy in the laboratory frame of 200 MeV. For the $D^0 \to K^-\pi^+\pi^0$ decay we select the dominant resonant contributions with a requirement on the Dalitz density distribution [9].

Finally, the D^+ and D^0 candidates are required to have an invariant mass within 2σ of the mean values. The D^+ and D^0 mass resolutions are mode-dependent and range between 5 and 8 MeV/c^2. We form D^{*+} candidates by combining D^0 candidates with charged tracks. The mass difference between the D^{*+} and the D^0 candidates is required to be within 2σ of the mean value as estimated on control samples. The resolution is mode-dependent, approximately 0.6 MeV/c^2 in all cases. We combine D^+
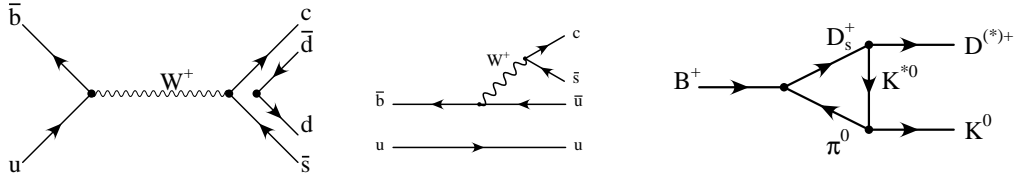
FIG. 1: Annihilation diagram for the decay $B^+ \to D^{(*)+} K_S^0$(left), tree diagram for $B^+ \to D_s^{(*)+} \pi^0$(center), and hadron-level diagram for a possible rescattering contribution to $B^+ \to D^{(*)+} K_S^0$ via $B^+ \to D_s^{(*)+} \pi^0$(right).

or D^{*+} candidates with a K_s^0 to form B^+ candidates. To improve the resolution on the four-momentum of all the intermediate composite particles we apply a kinematic fitting technique that constrains their masses to the nominal value [10] and their charged daughters to come from the same vertex.

We only accept events with a reconstructed candidate and a total measured energy greater than 4.5 GeV, determined using all charged tracks and neutral clusters in the electromagnetic calorimeter with energy above 30 MeV. The remaining background comes predominantly from continuum $q\bar{q}$ production. This background is suppressed using variables that characterize the topology of the event. We require the ratio of the second and zeroth order Fox-Wolfram moments [11] to be less than 0.5. We compute the angle θ_T between the thrust axis of the B-meson candidate and the thrust axis of the rest of the event. The thrust axis is defined as the direction that maximizes the sum of the longitudinal momenta of the particles in the center-of-mass (c.m.) frame. In this frame $B\bar{B}$ pairs are produced approximately at rest and have a uniform $|\cos\theta_T|$ distribution. In contrast, $q\bar{q}$ pairs are produced back-to-back, which results in a $|\cos\theta_T|$ distribution that peaks at unity. To further suppress backgrounds we use a Fisher discriminant $\mathcal{F}$ constructed from the scalar sum of the c.m. momenta of all tracks and photons, excluding the B candidate decay products, flowing into nine concentric cones centered on the thrust axis of the B candidate [12]. The more spherical the event, the lower the value of $\mathcal{F}$. Figure 2 shows the distribution of $\mathcal{F}$ and $|\cos\theta_T|$ on signal MC and on off-resonance data, which contain exclusively continuum $q\bar{q}$ production events. We also exploit the charge correlation between the B and the leptons and kaons produced in its decays to classify the events in three mutually exclusive categories with different levels of contamination from continuum background: events with at least one lepton with charge opposite to the B candidate, events with no lepton and at least one kaon among the tracks that do not form the B candidate but have opposite charge, and all the other events. The optimization of the selection is performed separately for each decay mode and for the three categories by maximizing the ratio of signal effi-

ciency, estimated with MC, over the square-root of the expected number of background events, estimated in data sidebands: the maximum allowed value of $|\cos\theta_T|$ ranges between 0.8 to 1 (i.e. no cut) and the maximum allowed value for $\mathcal{F}$ varies from 0.1 to 0.7.
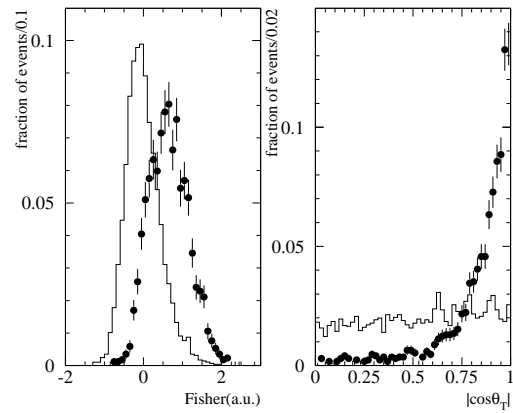

FIG. 2: Distribution of the discriminating variables $|\cos\theta_T|$ and $\mathcal{F}$ in the $B^+ \to D^+ K_s^0$ signal MC (histograms) and the off-resonance data (dots).

We extract the signal using the kinematic variables $m_{ES} = \sqrt{E_b^{*2} - (\sum_i \mathbf{p}_i^*)^2}$ and $\Delta E = \sum_i \sqrt{m_i^2 + \mathbf{p}_i^{*2}} - E_b^*$, where E_b^* is the beam energy in the c.m. frame, $\mathbf{p}_i^*$ is the c.m. momentum of daughter particle i of the B meson candidate, and m_i is the mass hypothesis for particle i. For signal events, m_{ES} peaks at the B meson mass with a resolution of about 2.5 MeV/c^2 and ΔE peaks near zero, indicating that the B candidate's total energy is consistent with the beam energy in the c.m. frame. The ΔE signal band is defined as $|\Delta E| < 2.5\sigma$ and within it we define the signal region as $5.2725 < m_{ES} < 5.2875$ GeV/c^2 and the m_{ES} sideband region as $5.2000 < m_{ES} < 5.2725$ GeV/c^2. The ΔE resolution σ is mode-dependent and approximately 18 MeV. We also define the ΔE sideband region as $2.5\sigma < |\Delta E| < 0.12$ GeV and $5.2 < m_{ES} < 5.3$ GeV/c^2. Table I shows the efficiency for each sub-decay mode estimated with simulated events. Depending on the mode, in 1.5 to 7% of the events there is more than

TABLE I: Efficiencies for the $B^+ \to D^{(*)+}K_s^0$ candidate reconstruction in each sub-decay mode. The branching fraction of the $D^{(*)+}$ decay chains considered [10] are also shown.

D mode	$\varepsilon_i(\%)$	B(%)
$D^+ \to K_S^0\pi^+$; $K_S^0 \to \pi^-\pi^+$	17.3	0.97 ± 0.06
$D^+ \to K^-\pi^+\pi^+$	17.7	9.2 ± 0.6
$D^{*+} \to D^0\pi^+$;		
$\quad D^0 \to K^-\pi^+$	18.5	2.57 ± 0.06
$\quad D^0 \to K^-\pi^+\pi^0$	6.4	8.8 ± 0.5
$\quad D^0 \to K^-\pi^+\pi^-\pi^+$	10.1	5.05 ± 0.21
$\quad D^0 \to K_S^0\pi^+\pi^-$; $K_S^0 \to \pi^-\pi^+$	10.6	1.37 ± 0.08

FIG. 3: The $m_{\rm ES}$ distribution for the a) $B^+ \to D^+K_s^0$ and b) $B^+ \to D^{*+}K_s^0$ candidates within the ΔE signal band in data after all selection requirements. Combinatorial (full line) and peaking (dashed line) backgrounds are superimposed.

one B candidate. We select the B candidate whose $D^{(*)}$ candidate's mass is closest to its nominal mass or, in case two B candidates are formed by the same the $D^{(*)}$ candidate, one with the smallest value of $|\Delta E|$.

After the selection described above, two classes of backgrounds remain. First, there is *combinatorial background* in the signal region, coming from random combinations of tracks in the event. We estimate this background from the sideband of the m_{ES} distribution, describing it with a threshold function $dN/dm_{ES} \propto m_{ES}\sqrt{1 - m_{ES}^2/E_b^{*2}}\exp\left[-\xi\left(1 - m_{ES}^2/E_b^{*2}\right)\right]$, characterized by the shape parameter ξ [13]. We obtain the parameter ξ from a fit to the distributions of m_{ES} in data, in the ΔE sideband region. The number of combinatorial background events is obtained by scaling the events in the sideband of the m_{ES} distribution into the signal region with the ratio of the threshold function area in the two regions. Including systematic errors, we estimate 56.3 ± 3.0 and 22.0 ± 1.8 events for the $B^+ \to D^+K_s^0$ and $B^+ \to D^{*+}K_s^0$ mode, respectively. Second, there is *peaking background* due to misreconstructed B meson decays that have an m_{ES} distribution peaking near the B mass. We study the peaking background with MC and we estimate it to be 4.4 ± 1.2 and 1.2 ± 0.6 events for the $B^+ \to D^+K_s^0$ and $B^+ \to D^{*+}K_s^0$ modes, respectively. The dominant contribution to the peaking background comes from well-known $B^0 \to D^{(*)-}X^+$ decays ($X^+ = \pi^+$, ρ^+, a_1^+). As a cross-check, we also estimate the peaking background using candidates from the D mass sidebands in data and we find results consistent with the MC prediction.

Figure 3 shows the m_{ES} distributions in the ΔE signal band for the two modes after the selection. The expected background is superimposed.

To compute the confidence level (C.L.) at which the data agree with a given hypothesis on $\mathcal{B}(B^+ \to D^{(*)+}K^0)$ we use a frequentist technique [14], which treats properly the small number of events and includes the systematic errors directly in the computation of confidence intervals or limits. The C.L. is defined as the fraction of times a random number, following the expected dis-
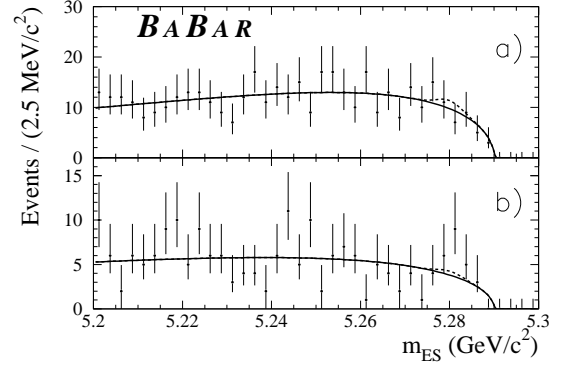
tribution of the number of events in the signal region (N_{exp}), exceeds the number of observed events (N_{cand} in Tab. II). N_{exp} is distributed according to the sum of Poissonian distributions with mean values μ distributed as follows: for a given value of $\mathcal{B}(B^+ \to D^{(*)+}K^0)$ we estimate μ as the sum of the expectation value of the number of events from the combinatorial and peaking background (N_{comb} and N_{peak}, respectively), and from the signal (N_{sig}), $\mu = N_{comb} + N_{peak} + N_{sig}$.

We estimate N_{comb} by scaling the number of events in the m_{ES} sideband to the signal region and by considering the Poisson fluctuations of the number of events in the sideband and the systematic uncertainties on the threshold parameter ξ. We estimate N_{peak} from the MC, taking into account its limited statistics. Table II reports the mean values and standard deviations for N_{comb} and N_{peak}. Finally, for a given value of the branching fraction, N_{sig} is obtained as:

$$N_{sig} = \mathcal{B}(B^+ \to D^{(*)+}K^0) \times N_B \times \Sigma_i\epsilon_i\mathcal{B}_i \quad (1)$$

where the number of $B^\pm$ mesons (N_B) and the product of the efficiency and the branching fraction of the

TABLE II: The number of candidates in the signal region in data ($N_{\rm cand}$), the corresponding expected combinatorial background ($N_{\rm comb}$), the peaking background ($N_{\rm peak}$), the probability (P_{bkgd}) of the data being consistent with the background fluctuating up to the level of the data in absence of signal, and the 90% confidence-level upper limit. Systematic uncertainties are included.

B mode	$N_{\rm cand}$	$N_{\rm comb}$	$N_{\rm peak}$	$P_{bkgd}(\%)$	90% C.L.
$D^+ \ K_s^0$	57	56.3 ± 3.0	4.4 ± 1.2	69	0.5×10^{-5}
$D^{*+} \ K_s^0$	28	22.0 ± 1.8	1.2 ± 0.6	24	0.9×10^{-5}

sub-decay modes ($\Sigma_i \epsilon_i \mathcal{B}_i$) are varied according to Gaussian distributions within their systematic uncertainties. The systematic errors on the reconstruction efficiency are shown in Table III and include the uncertainty due to limited MC statistics, uncertainty on tracking efficiency, K_s^0 and π^0 reconstruction, charged-kaon identification, other selection criteria. They have all been estimated by comparing the data and simulation performances in control samples. Also, the uncertainties on N_B (1.1%) and on the branching fraction of the sub-decay modes have been taken into account. The total uncertainty is obtained by adding the contributions from the individual sources in quadrature.

Calculating the C.L. with the procedure just described and setting $\mathcal{B}(B^+ \to D^{(*)+} K^0) = 0$, we estimate the probability of the background to fluctuate above the observed number of events to be 69% and 24% for the $B^+ \to D^+ K_s^0$ and for the $B^+ \to D^{*+} K_s^0$ modes, respectively. In absence of significant signal we then set the following upper limits on the values of the branching fractions corresponding to a C.L. of 90%:

$$\mathcal{B}(B^+ \to D^+ K^0) \;<\; 0.5 \times 10^{-5}, \qquad (2)$$
$$\mathcal{B}(B^+ \to D^{*+} K^0) \;<\; 0.9 \times 10^{-5}.$$

We also compute the branching fractions $\mathcal{B}(B^+ \to D^+ K^0) = (-0.28^{+0.61}_{-0.56}) \times 10^{-5}$ and $\mathcal{B}(B^+ \to D^{*+} K^0) = (0.28^{+0.44}_{-0.41}) \times 10^{-5}$. The errors above include both the statistical and the systematic uncertainties.

In conclusion, we report on the search for the rare decays $B^+ \to D^{(*)+} K_s^0$, which are predicted to proceed through annihilation diagrams. We do not observe any significant signal and we set 90% C.L. upper limits on their branching fractions.

[*] Also with Università della Basilicata, Potenza, Italy
[†] Deceased
[1] M. Battaglia et al., Proceedings of the 1st CKM Workshop, "The CKM Matrix and the Unitarity Triangle" 13-16 February (2002) CERN (Geneva), Yellow-Book Report, CERN-2003-002-corr, 10 October 2003, [hep-ph/0304132], pag.147.
[2] B. Blok, M. Gronau and J. L. Rosner, Phys. Rev. Lett. **78**, 3999 (1997).
[3] Charge conjugation is implied throughout this letter.
[4] A. J. Buras, L. Silvestrini, Nucl. Phys.B **569**, 3 (2000).
[5] M. Gronau, D. London, Phys. Lett. B **253**, 483 (1991).
[6] CLEO Collaboration, A. Gritsan et al. , Phys. Lett. D **64**, 077501 (2001).
[7] BABAR Collaboration, B. Aubert et al., Nucl. Instr. and Methods **A479**, 1 (2002).
[8] GEANT4 Collaboration, S. Agostinelli et al., Nucl. Instr. and Methods **A506**, 250 (2003).
[9] E687 Collaboration, P. L. Frabetti et al., Phys. Lett. B **331**, 217 (1994).
[10] Particle Data Group, S.Eidelman et al., Phys. Lett. B **592**, 1 (2004).
[11] G.C. Fox and S. Wolfram, Phys. Rev. Lett. **41**, 1581 (1978).
[12] BABAR Collaboration, B. Aubert et al., Phys. Rev. Lett. **87**, 151802 (2001).
[13] ARGUS Collaboration, H. Albrecht et al., Z. Phys. C **48**, 543 (1990).
[14] See for instance Ref. [10], section 32.3.2

TABLE III: Relative systematic errors on the branching fraction due to, respectively: MC statistics , track reconstruction , Kaon identification, K_s^0 and π^0 reconstruction efficiencies, and the data-MC agreement on the signal shapes of ΔE, $\cos\theta_T$, and $\mathcal{F}$.

D mode	MC(%)	Tracks(%)	Kaon(%)	K_s^0(%)	π^0(%)	ΔE(%)	$\cos\theta_T$(%)	$\mathcal{F}$(%)	Total(%)
$D^+ \to K_s^0 \pi^+$	1.4	1.1	-	0.3	-	0.4	0.4	0.7	2.0
$D^+ \to K^- \pi^+ \pi^+$	0.5	1.1	0.4	0.2	-	0.4	0.4	0.7	1.5
$D^0 \to K^- \pi^+$	0.9	1.2	0.4	0.2	-	0.8	0.4	0.7	1.8
$D^0 \to K^- \pi^+ \pi^0$	0.3	0.4	0.1	0.1	0.3	0.2	0.1	0.3	0.7
$D^0 \to K^- \pi^+ \pi^- \pi^+$	0.5	0.9	0.2	0.1	-	0.1	0.2	0.4	1.2
$D^0 \to K_S^0 \pi^+ \pi^-$	1.0	1.0	-	0.2	-	0	0.2	0.4	1.5